Applied and
Computational
Mechanics

Mathematical modelling of friction-vibration interactions of nuclear fuel rods

V. Zeman[a,*], Z. Hlaváč[a]

[a]*NTIS – New Technologies for Information Society, Faculty of Applied Sciences, University of West Bohemia, Univerzitní 8, 306 14 Plzeň, Czech Republic*

Abstract

Nuclear fuel rods (FRs) are transversely linked to each other by three spacer grid cells at several vertical levels inside a fuel assembly (FA). Vibration of FA components, caused by the motion of FA support plates in the reactor core, generates variable contact forces between FRs and spacer grid cells. Friction effects in contact surfaces have an influence on the expected lifetime period of nuclear FA in terms of FR cladding fretting wear. This paper introduces an original approach to mathematical modelling and simulation analysis of FR nonlinear vibrations and fretting wear taking into consideration friction forces at all levels of spacer grids.
© 2016 University of West Bohemia. All rights reserved.

Keywords: nuclear fuel rod, friction-vibration interactions, friction work, fretting wear

1. Introduction

Friction in mechanical systems has been systematicaly investigated for over half a millenia. The historical backround is presented in detail, for example, in book [2]. In terms of mechanics, a nuclear fuel assembly is a very complicated system of beam-type componets [1, 4]. The basic structure (Fig. 1) is formed by a large number of parallel vertically distributed FRs, some guide thimbles and a centre tube. The FRs are linked to each other by transverse spacer grids (SGs) and with load-bearing skeleton by means of lower piece. Vibration of nuclear FA in consideration of complexity [19–21] was investigated using a linear system with proportional damping. Application of these mathematical models enables approximate calculation of friction forces between FR and SG cells during slip motion without the consideration of possible stick phases and elastic deformations of SG cells in tangential and vertical directions. To achieve more exact results, computational friction-vibration analyses of FRs should be based on more sophisticated computational friction models with "force-slip velocity-displacement" characteristics. This approach is theoretically introduced, for example, in [14, 15] including the effect of surface roughness.

The authors of the present paper have investigated the modelling of VVER-type reactors in co-opration with the Nuclear Research Institute Řež and Škoda Nuclear Machinery for more than three decades. The original linearised spatial model of the VVER-1000/320-type reactor, intended for eigenvalues and dynamic response calculation excited by pressure pulsations, was derived during the year 2006 [17]. The reactor model was used for the calculation of the spatial motion of FA lower support plate in core barrel bottom and upper support plate in block of protection tubes [18] and it was partially experimentally verified in [11]. The source of FA kinematic excitation is the support plates motion excited by pressure pulsations generated by

---

*Corresponding author. Tel.: +420 377 632 332, e-mail: zemanv@kme.zcu.cz.
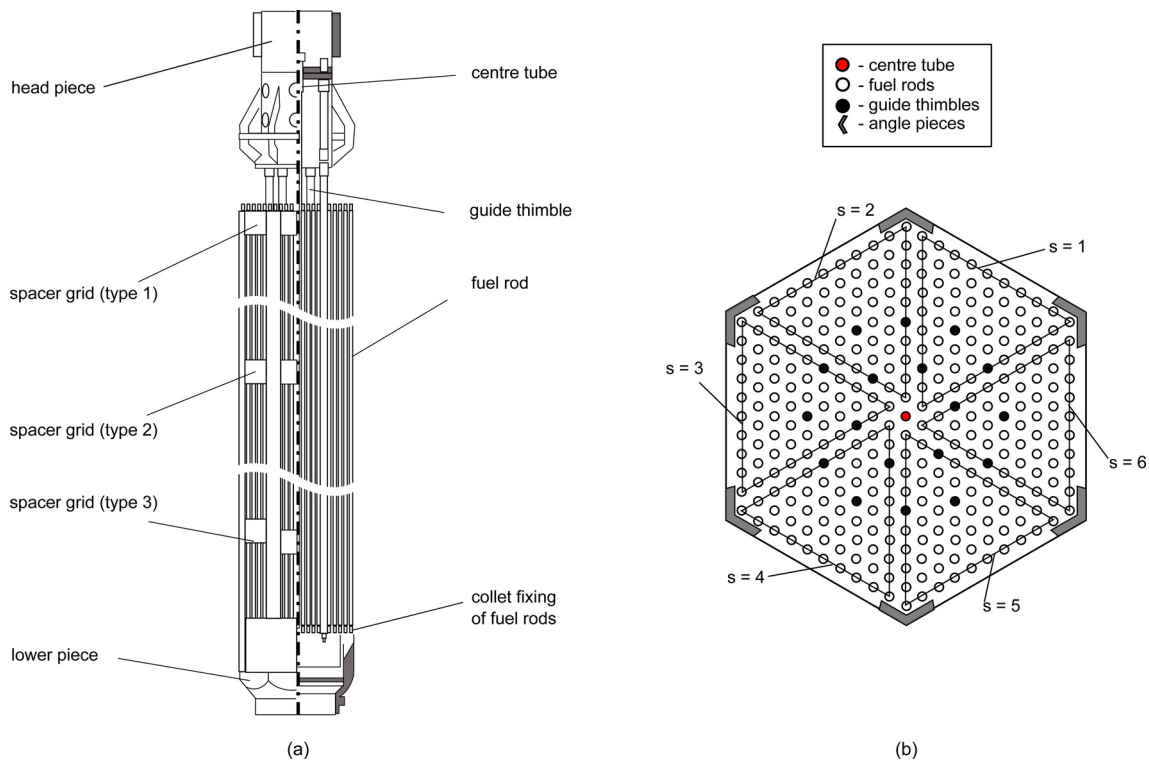
Fig. 1. FA schematic side view (a) and the cross-section of FA (b)

main circulation pumps in the coolant loops of the reactor primary circuit. The modelling of the FA vibration based on the modal synthesis method with reduction of the DOF number and under the assumption of full interaction of all FA components was presented in several research reports, monograph [4], and papers [19, 20] published by the authors of the present paper.

The vibration induced by pressure pulsation in the reactor, in particular at the contact points between the spacer grid cells and FR, may result in wear of the fuel rod cladding. This phenomenon can lead to exposure of fuel pellets [10]. The majority of published papers on fretting wear of rods deals with experimental investigation of friction work per unit area which is converted into wear depth during a certain time interval [3] by means of the wear coefficient. The calculation of friction work is based on the estimation of average normal contact force, fretting amplitude and oscillation frequency. This approach does not respect the time dependence of normal contact forces and the possible temporary loss of fretting contact [9]. Several works focus on the influence of chosen parameters on fretting wear. In this context, the influence of geometry and elastic properties of SG is very important [5,7,8]. In [13], a probabilistic prediction of fretting wear of nuclear FRs is presented. Other papers are motivated by problems of fretting wear that occur during reactor operation at the power plants [6, 16, 22].

The aim of this paper is the investigation of nonlinear kinematically excited spatial vibration of a chosen FR (Fig. 2) and its fretting wear taking into consideration the friction-vibration interactions in all contact surfaces between FR and SG cells.

2. Dynamic model of the fuel rod

Let us consider a chosen fuel rod u in the segment s (see Fig. 1b) which is fixed at the level of the nodal point $L_u^{(s)}$ into the mounting plane (see Fig. 2a) in reactor core barrel bottom.
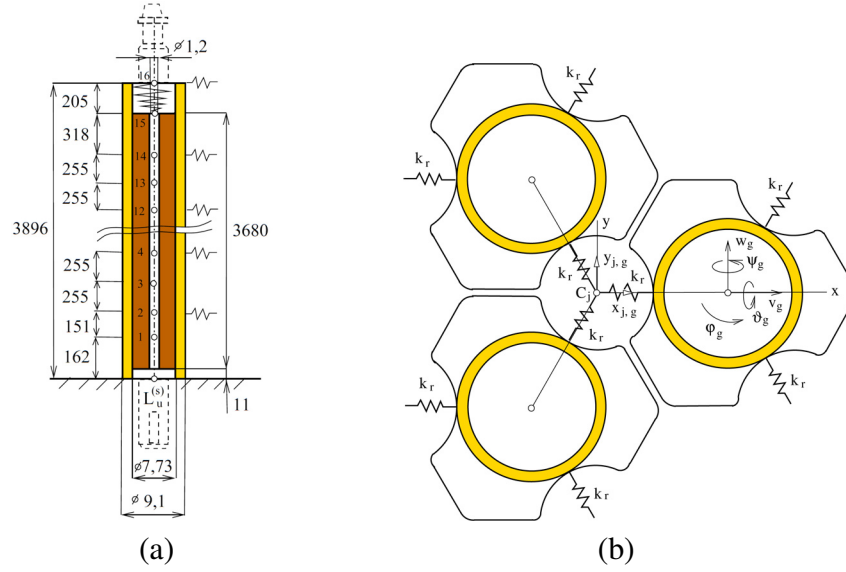
Fig. 2. FR model (a) and the cross-section of SG cells segment (b)

Each FR is surrounded by three SG cells at every level $g = 2i$, Fig. 2b. The elastic properties of one cell in horizontal plane are expressed by three springs of identical radial stiffness k_r located between the cell centres C_j, $j = 1, 2, 3$ and three FRs in contact. The displacements of cell centres $x_{j,g}$ and $y_{j,g}$ in the directions of horizontal axes x, y were investigated with the simplifying assumption of modal damping using the global FA model [4, 20]. FA vibrations are excited by pressure pulsations generated by main circulation pumps in the coolant loops of the reactor primary circuit.

The main components of the FR are a thin-walled tube from zirconium (father FR cladding) and fuel pellets from UO_2. The compact form of a fuel pellets column is held by means of inside pressed fixation spring at the top of FR (see Fig. 2a). We assume a full interaction of both FR components during a fixed period of reactor operation.

The FR mathematical model of beam type is derived by FEM for Euler-Bernoulli continua including mass forces on flexure (Rayleigh theory) in the configuration space

$$\boldsymbol{q} = [\dots, u_i, v_i, w_i, \varphi_i, \vartheta_i, \psi_i, \dots]^T, \quad i = L_u^{(s)}, 1, \dots, 16, \tag{1}$$

where u_i is axial displacement and v_i, w_i are mutually perpendicular lateral displacements of the central nodal point i in the direction of axes x, y. The angular displacements φ_i, ϑ_i, ψ_i are torsional and bending angles of rod cross-section around the vertical z and lateral axes $x_i \parallel x$, $y_i \parallel y$, respectively, at the level of nodal points i. The even nodes $i = 2, \dots, 16$ are at the level of spacer grid g (see Fig. 2) and the odd nodes are located in the middle.

The mathematical model of a spatially vibrating FR is derived in the decomposed block form

$$\begin{bmatrix} \boldsymbol{M}_L & \boldsymbol{M}_{L,F} \\ \boldsymbol{M}_{F,L} & \boldsymbol{M}_F \end{bmatrix} \begin{bmatrix} \ddot{\boldsymbol{q}}_{L_u}^{(s)} \\ \ddot{\boldsymbol{q}}_F \end{bmatrix} + \begin{bmatrix} \boldsymbol{B}_L & \boldsymbol{B}_{L,F} \\ \boldsymbol{B}_{F,L} & \boldsymbol{B}_F \end{bmatrix} \begin{bmatrix} \dot{\boldsymbol{q}}_{L_u}^{(s)} \\ \dot{\boldsymbol{q}}_F \end{bmatrix} + \begin{bmatrix} \boldsymbol{K}_L & \boldsymbol{K}_{L,F} \\ \boldsymbol{K}_{F,L} & \boldsymbol{K}_F \end{bmatrix} \begin{bmatrix} \boldsymbol{q}_{L_u}^{(s)} \\ \boldsymbol{q}_F \end{bmatrix} = \begin{bmatrix} \boldsymbol{f}_L \\ \boldsymbol{f}_{C,FR} \end{bmatrix}, \tag{2}$$

where displacements of the node $L_u^{(s)}$ (coupled with the mounting plate) are integrated into the subvector $\boldsymbol{q}_{L_u}^{(s)} \in R^6$ and displacements of the nodes $i = 1, \dots, 16$ are integrated into the subvector $\boldsymbol{q}_F \in R^{96}$. The force subvector $\boldsymbol{f}_L \in R^6$ stands for forces acting in the kinematically excited node $L_u^{(s)}$. The force subvector $\boldsymbol{f}_{C,FR} \in R^{96}$ expresses the coupling forces between the

surrounding spacer grid cells and FR at the level of all spacer grids $g = 1, \ldots, 8$ (level of the even nodes). The second set of equations extracted from the FR model in the decomposed form (2) can be written as

$$\boldsymbol{M}_F \ddot{\boldsymbol{q}}_F + \boldsymbol{B}_F \dot{\boldsymbol{q}}_F + \boldsymbol{K}_F \boldsymbol{q}_F = -\boldsymbol{M}_{F,L} \ddot{\boldsymbol{q}}_{L_u}^{(s)} - \boldsymbol{B}_{F,L} \dot{\boldsymbol{q}}_{L_u}^{(s)} - \boldsymbol{K}_{F,L} \boldsymbol{q}_{L_u}^{(s)} + \boldsymbol{f}_{C,FR}. \tag{3}$$

The first three terms on the right-hand side express the kinematic excitation by the lower FA mounting plate motion calculated from the global reactor model [18].

3. Contact forces between FR and spacer grid cells

The contact forces between FR and the surrounding spacer grid cells in each contact point can be expressed by three components: normal $N_{j,g}$, tangential $T_{j,g}$ and axial $A_{j,g} \parallel z$ (Fig. 3). The dry friction is described by the force-slip velocity-displacement characteristics. The spacer grid cells are static preloaded and the FA vibrates with small relative displacements with regard to the cells.
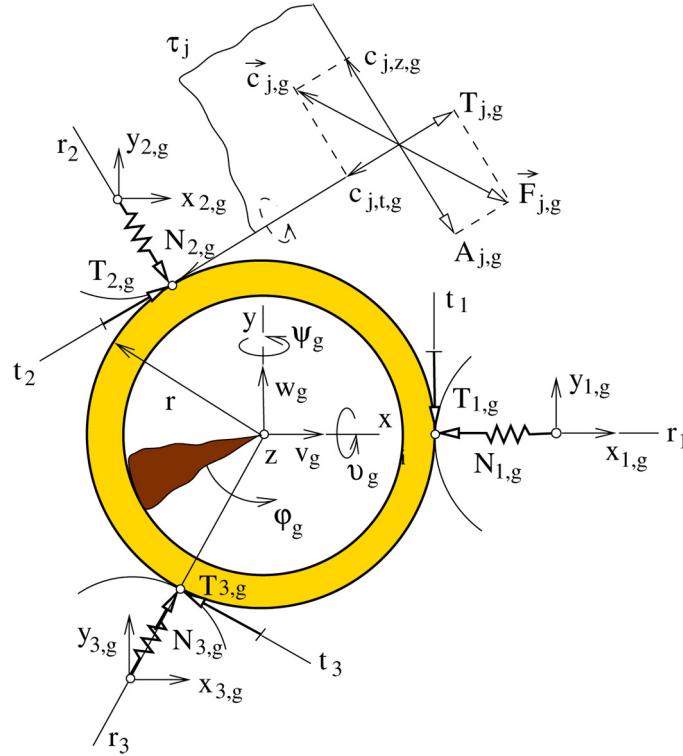

Fig. 3. FR cross-section at the level of SG g

Sliding shifts and velocities of FR cladding in the contact points (contact surfaces are very small) with surrounding SG cells $j = 1, 2, 3$ at the level of spacer grids $g = 1, \ldots, 8$ are generated as a result of FR spatial vibrations inside the FA load-bearing skeleton with spacer grids. These relative shifts of the FR cladding in radial (r), tangential (t) and axial (z) directions (the axes $r_j, t_j, z_j \parallel z$ form a right-handed coordinate system in contact points) can be expressed in the form

$$d_{1,r,g} = v_g - x_{1,g},$$
$$d_{2,r,g} = -0.5(v_g - x_{2,g}) + \frac{\sqrt{3}}{2}(w_g - y_{2,g}), \tag{4}$$

$$d_{3,r,g} = -0.5(v_g - x_{3,g}) - \frac{\sqrt{3}}{2}(w_g - y_{3,g}),$$

$$d_{1,t,g} = w_g - y_{1,g} + r\varphi_g,$$

$$d_{2,t,g} = -\frac{\sqrt{3}}{2}(v_g - x_{2,g}) - 0.5(w_g - y_{2,g}) + r\varphi_g, \tag{5}$$

$$d_{3,t,g} = \frac{\sqrt{3}}{2}(v_g - x_{3,g}) - 0.5(w_g - y_{3,g}) + r\varphi_g,$$

$$d_{1,z,g} = u_g - r\psi_g - z_{1,g},$$

$$d_{2,z,g} = u_g + r\frac{\sqrt{3}}{2}\vartheta_g + 0.5r\psi_g - z_{2,g}, \tag{6}$$

$$d_{3,z,g} = u_g - r\frac{\sqrt{3}}{2}\vartheta_g + 0.5r\psi_g - z_{3,g},$$

where r is outer radius of FR cladding and $u_g, v_g, w_g, \varphi_g, \vartheta_g, \psi_g$ are FR displacements of the central nodal point at the level of spacer grid g. The small vertical displacements $z_{j,g}$ of the cell centres, in consequence of large vertical FA skeleton stiffness, can be approximately expressed as identical to the vertical displacement of the FA lower mounting plate in the intersection point with the FR vertical axis ($z_{j,g} \approx u_{L_u}^{(s)}$, see relation (19))

$$z_{j,g} = z_L + \eta\varphi_{x,L} - \xi\varphi_{y,L}. \tag{7}$$

The components of sliding velocities $c_{j,t,g} = \dot{d}_{j,t,g}$ and $c_{j,z,g} = \dot{d}_{j,z,g}$ in tangential planes τ_j ($j = 1, 2, 3$) are expressed by time derivatives of corresponding shifts (see Fig. 3).

The mathematical model of the friction-vibration interactions generally takes into consideration three states [15] — *stick, slip* and *separation* — depending on the slip velocity and the normal contact force. Taking into account the relationship between the friction coefficient f, sliding velocity $c_j = \sqrt{c_{j,t}^2 + c_{j,z}^2}$ and relative FR shifts $d_{j,r}, d_{j,t}, d_{j,z}$ in radial, tangential and axial directions, respectively, the conditions for the above mentioned states can be formulated as follows (index g is omitted):

$$\text{– stick conditions} \ldots |c_j| = 0, \ T_j = k_t d_{j,t}, \ A_j = k_z d_{j,z}, \tag{8}$$

$$\text{– slip conditions} \ldots |c_j| > 0, \ \vec{F_j} = -f(c_j)N_j\frac{\vec{c_j}}{|c_j|}, \tag{9}$$

$$\text{– separation conditions} \ldots N_j = N_0 + k_r d_{j,r} \leq 0. \tag{10}$$

Here N_j, T_j, A_j are the components of the resulting contact force in negative radial, tangential and axial directions (Fig. 3). The static contact force N_0 stands for the preloading between FR and particular spacer grid cells and $\vec{F_j}$ is friction force.

The elastic properties of cells are expressed by radial k_r, tangential k_t and axial k_z stiffnesses ($k_t, k_z > k_r$) in relation to cell centres. The mathematical model of the contact forces components at the level of the spacer grid $g = 1, \ldots, 8$ including all three states can be approximated by the functions

$$N_{j,g} = (N_0 + k_r d_{j,r,g})H(N_0 + k_r d_{j,r,g}), \tag{11}$$

$$T_{j,g} = f(c_{j,g})N_{j,g}\frac{c_{j,t,g}}{c_{j,g}} + k_t(c_{j,g})d_{j,t,g}, \tag{12}$$

$$A_{j,g} = f(c_{j,g})N_{j,g}\frac{c_{j,z,g}}{c_{j,g}} + k_z(c_{j,g})d_{j,z,g}, \tag{13}$$

where $c_{j,g}$ are the resulting slip velocities. The Heaviside function H in (11) is zero for negative values of $N_0 + k_r d_{j,r,g}$ (separation state), where N_0 is static preloading of spacer grid cells about the radial stiffness k_r. The approximative smooth function for the friction coefficient has to satisfy the conditions $f(c_{j,g}) \leq f_{st}$ for $0 \leq |c_{j,g}| < c_{krit}$ and $f_d \leq f(c_{j,g}) < f_{st}$ for $|c_{j,g}| > c_{krit}$, where c_{krit} is the critical sliding velocity separating the stick-state (phase of microslip) from the slip-state (phase of macroslip) and f_{st} and f_d are the static and dynamic friction coefficients, respectively. The approximative functions for cell stiffnesses in tangential and axial directions satisfy the conditions $k_t(c_{j,g}) \approx k_t$, $k_z(c_{j,g}) \approx k_z$ for $0 \leq |c_{j,g}| < c_{krit}$ and $k_t(c_{j,g}) \ll k_t$, $k_z(c_{j,g}) \ll k_z$ for $|c_{j,g}| > c_{krit}$. The smooth functions

$$f(c_{j,g}) = \frac{2}{\pi} \arctan(\varepsilon_f c_{j,g})[f_d + (f_{st} - f_d)e^{-dc_{j,g}}] \tag{14}$$

and

$$k_t(c_{j,g}) = k_t e^{-(\varepsilon_k c_{j,g})^2}, \quad k_z(c_{j,g}) = k_z e^{-(\varepsilon_k c_{j,g})^2} \tag{15}$$

approximately satisfy the required conditions for suitably selected parameters f_{st}, f_d, ε_f, ε_k, d.

The contact forces componets in particular contact points $j = 1, 2, 3$ must be transformed into FR nodes at each level of spacer grids $g = 1, \ldots, 8$ as

$$\boldsymbol{f}_{1,g} = \begin{bmatrix} -A_{1,g} \\ -N_{1,g} \\ -T_{1,g} \\ -T_{1,g}r \\ 0 \\ A_{1,g}r \end{bmatrix}, \quad \boldsymbol{f}_{2,g} = \begin{bmatrix} -A_{2,g} \\ 0.5N_{2,g} + \frac{\sqrt{3}}{2}T_{2,g} \\ -\frac{\sqrt{3}}{2}N_{2,g} + 0.5T_{2,g} \\ -rT_{2,g} \\ -\frac{\sqrt{3}}{2}rA_{2,g} \\ -0.5rA_{2,g} \end{bmatrix}, \quad \boldsymbol{f}_{3,g} = \begin{bmatrix} -A_{3,g} \\ 0.5N_{3,g} - \frac{\sqrt{3}}{2}T_{3,g} \\ \frac{\sqrt{3}}{2}N_{3,g} + 0.5T_{3,g} \\ -rT_{3,g} \\ \frac{\sqrt{3}}{2}rA_{3,g} \\ -0.5rA_{3,g} \end{bmatrix}. \tag{16}$$

The force subvector $\boldsymbol{f}_{C,FR}$ in the FR mathematical model (3), in accordance with the vector of FR generalized coordinates defined in (1), has the form

$$\boldsymbol{f}_{C,FR}(\boldsymbol{q}_F, \dot{\boldsymbol{q}}_F, t) = \sum_{j=1}^{3} [\boldsymbol{0}^T, \boldsymbol{f}_{j,1}^T, \ldots, \boldsymbol{0}^T, \boldsymbol{f}_{j,g}^T, \ldots, \boldsymbol{0}^T, \boldsymbol{f}_{j,8}^T]. \tag{17}$$

4. Nonlinear FR vibration excited by pressure pulsation

Let use consider the spatial motion of the lower FA mounting plate (MP) in the reactor core barrel bottom described in the fixed coordinate system x_{MP}, y_{MP}, z_{MP} with the origin in the plate gravity centre L in static equilibrium state by the displacement vector (see Fig. 4)

$$\boldsymbol{q}_L(t) = [x_L, y_L, z_L, \varphi_{x,L}, \varphi_{y,L}, \varphi_{z,L}]^T. \tag{18}$$

The vector of FR displacements in the lower end-node $L_u^{(s)}$ of the chosen FR coupled with the plate can be expressed according to (1) in the form

$$\begin{bmatrix} u \\ v \\ w \\ \varphi \\ \vartheta \\ \psi \end{bmatrix}_{L_u^{(s)}} = \begin{bmatrix} 0 & 0 & 1 & \eta & -\xi & 0 \\ 1 & 0 & 0 & 0 & \zeta & -\eta \\ 0 & 1 & 0 & -\zeta & 0 & \xi \\ 0 & 0 & 0 & 0 & 0 & 1 \\ 0 & 0 & 0 & 1 & 0 & 0 \\ 0 & 0 & 0 & 0 & 1 & 0 \end{bmatrix} \begin{bmatrix} x_L \\ y_L \\ z_L \\ \varphi_{x,L} \\ \varphi_{y,L} \\ \varphi_{z,L} \end{bmatrix}, \tag{19}$$
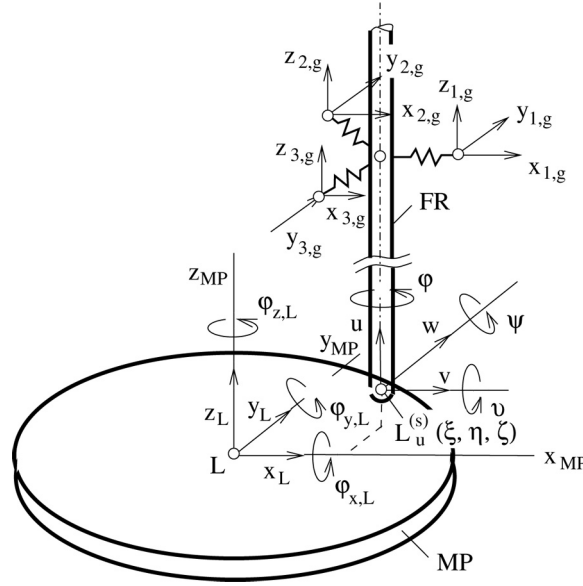
Fig. 4. Spatial motion of the lower FA mounting plate

or

$$\boldsymbol{q}_{L_u}^{(s)}(t) = \boldsymbol{T}_{u,L}^{(s)}\boldsymbol{q}_L(t), \tag{20}$$

where ξ, η, ζ are the coordinates of the FR centre $L_u^{(s)}$ in the coordinate system x_{MP}, y_{MP}, z_{MP}. The FR kinematic excitation in (3) by the mounting plate motion can be expressed in the form of the force vector

$$\boldsymbol{f}_{L_u}^{(s)}(t) = -\boldsymbol{M}_{F,L}\boldsymbol{T}_{u,L}^{(s)}\ddot{\boldsymbol{q}}_L(t) - \boldsymbol{B}_{F,L}\boldsymbol{T}_{u,L}^{(s)}\dot{\boldsymbol{q}}_L(t) - \boldsymbol{K}_{F,L}\boldsymbol{T}_{u,L}^{(s)}\boldsymbol{q}_L(t). \tag{21}$$

The steady-state vibration of the reactor excited by coolant pressure pulsation generated by the main circulation pumps were investigated in co-operation with NRI Řež and published in [18]. The dynamic response of the FA mounting plate was expressed in the complex form

$$\tilde{\boldsymbol{q}}_L(t) = \sum_l \sum_k \tilde{\boldsymbol{q}}_{L,l}^{(k)} \mathrm{e}^{\mathrm{i}k\omega_l t}, \tag{22}$$

where $\tilde{\boldsymbol{q}}_{L,l}^{(k)}$ is vector of complex amplitudes of the plate gravity centre displacements defined in (18) excited by the kth harmonic component of the coolant pressure pulsations generated by one lth main circulation pump in corresponding cooling loops of the reactor primary circuit. Corresponding angular rotational frequency of the lth pump $\omega_l = 2\pi f_l$ is defined by pump revolutions, which can be slightly different for a particular pump of the cooling system. The excitation force vector defined in (21) can be expressed in the complex form

$$\tilde{\boldsymbol{f}}_{L_u}^{(s)}(t) = \sum_l \sum_k \tilde{\boldsymbol{f}}_{l,k} \mathrm{e}^{\mathrm{i}k\omega_l t}, \tag{23}$$

where the vectors of complex amplitudes are

$$\tilde{\boldsymbol{f}}_{l,k} = (k^2\omega_l^2\boldsymbol{M}_{F,L} - \mathrm{i}k\omega_l\boldsymbol{B}_{F,L} - \boldsymbol{K}_{F,L})\boldsymbol{T}_{u,L}^{(s)}\tilde{\boldsymbol{q}}_{L,l}^{(k)}. \tag{24}$$

The real force vector defined in (21) can be rewritten as

$$\boldsymbol{f}_{L_u}^{(s)}(t) = \sum_l \sum_k \left(\mathrm{Re}[\tilde{\boldsymbol{f}}_{l,k}] \cos k\omega_l t - \mathrm{Im}[\tilde{\boldsymbol{f}}_{l,k}] \sin k\omega_l t \right). \tag{25}$$

The lateral displacements $x_{j,g}$ and $y_{j,g}$, $j = 1, 2, 3$ of the cell centres apearing in (4) and (5) are calculated using the global FA model [20] as

$$x_{j,g} = \sum_l \sum_k \left(\overline{x}_{j,g,l}^{(k)} \cos k\omega_l t - \overline{\overline{x}}_{j,g,l}^{(k)} \sin k\omega_l t \right), \tag{26}$$

$$y_{j,g} = \sum_l \sum_k \left(\overline{y}_{j,g,l}^{(k)} \cos k\omega_l t - \overline{\overline{y}}_{j,g,l}^{(k)} \sin k\omega_l t \right) \tag{27}$$

from their complex amplitudes

$$\tilde{x}_{j,g,l}^{(k)} = \overline{x}_{j,g,l}^{(k)} + \mathrm{i}\overline{\overline{x}}_{j,g,l}^{(k)}, \quad \tilde{y}_{j,g,l}^{(k)} = \overline{y}_{j,g,l}^{(k)} + \mathrm{i}\overline{\overline{y}}_{j,g,l}^{(k)}. \tag{28}$$

The FR mathematical model (3) can be formally rewritten as

$$\boldsymbol{M}_F \ddot{\boldsymbol{q}}_F(t) + \boldsymbol{B}_F \dot{\boldsymbol{q}}_F(t) + \boldsymbol{K}_F \boldsymbol{q}_F(t) = \boldsymbol{f}_{L_u}^{(s)}(t) + \boldsymbol{f}_{C,FR}(\boldsymbol{q}_F, \dot{\boldsymbol{q}}_F, t). \tag{29}$$

The friction-vibration interactions of the FR cladding with spatially vibrating spacer grid cells are included in the nonlinear vector $\boldsymbol{f}_{C,FR}(\boldsymbol{q}_F, \dot{\boldsymbol{q}}_F, t)$ defined in (17). The dynamic response is investigated by integrating the equations of motion (29) in time domain transformed into 2×96 differential equations of the first order

$$\dot{\boldsymbol{u}} = \boldsymbol{A}\boldsymbol{u} + \boldsymbol{f}(\boldsymbol{u}, t), \tag{30}$$

where

$$\boldsymbol{u} = \begin{bmatrix} \boldsymbol{q}_F \\ \dot{\boldsymbol{q}}_F \end{bmatrix}, \quad \boldsymbol{A} = - \begin{bmatrix} \boldsymbol{0} & -\boldsymbol{E} \\ \boldsymbol{M}_F^{-1}\boldsymbol{K}_F & \boldsymbol{M}_F^{-1}\boldsymbol{B}_F \end{bmatrix},$$

$$\boldsymbol{f}(\boldsymbol{u}, t) = \begin{bmatrix} \boldsymbol{0} \\ \boldsymbol{M}_F^{-1}\left(\boldsymbol{f}_{L_u}^{(s)}(t) + \boldsymbol{f}_{C,FR}(\boldsymbol{q}_F, \dot{\boldsymbol{q}}_F, t) \right) \end{bmatrix}. \tag{31}$$

These equations are solved for initial conditions resulting from displacements and velocities of the lower FA mounting plate and undeformed FR in the initial moment of a simulation using the standard Runge-Kutta integration scheme in Matlab. Because of a large number of nonlinearities (number of contact points is $3 \times 8 = 24$) and three possible friction-vibration states in each contact point, the calculation in very time-consuming.

5. Prediction of the FR cladding fretting wear

The fretting wear of the FR cladding is a particular type of FR wear that is expected in nuclear FA [12, 13]. The tangential $c_{j,t,g}$ and axial $c_{j,z,g}$ components of the slip velocities in the contact points (see Fig. 3), as a result of FR spatial vibration inside of the FA load-bearing skeleton with spacer grids, can be expressed in compliance with (5) and (6) in the form

$$c_{1,t,g} = \dot{w}_g - \dot{y}_{1,g} + r\dot{\varphi}_g,$$

$$c_{2,t,g} = -\frac{\sqrt{3}}{2}(\dot{v}_g - \dot{x}_{2,g}) - 0.5(\dot{w}_g - \dot{y}_{2,g}) + r\dot{\varphi}_g, \tag{32}$$

$$c_{3,t,g} = \frac{\sqrt{3}}{2}(\dot{v}_g - \dot{x}_{3,g}) - 0.5(\dot{w}_g - \dot{y}_{3,g}) + r\dot{\varphi}_g,$$

$$c_{1,z,g} = \dot{u}_g - r\dot{\psi}_g - \dot{z}_{1,g},$$

$$c_{2,z,g} = \dot{u}_g + r\frac{\sqrt{3}}{2}\dot{\vartheta}_g + 0.5r\dot{\psi}_g - \dot{z}_{2,g}, \tag{33}$$

$$c_{3,z,g} = \dot{u}_g - r\frac{\sqrt{3}}{2}\dot{\vartheta}_g + 0.5r\dot{\psi}_g - \dot{z}_{3,g},$$

where $\dot{u}_g$, $\dot{v}_g$, $\dot{w}_g$, $\dot{\varphi}_g$, $\dot{\vartheta}_j$, $\dot{\psi}_g$ are components of the vector $\dot{\boldsymbol{q}}_F$ in order $12(g-1)+7,\ldots,$ $12(g-1)+12$, $g = 1,\ldots,8$. The small vertical velocities of the cell centres surrounding the chosen FR, due to the large axial stiffness of the FA skeleton, are approximated in compliance with (7) in the form

$$\dot{z}_{j,g} \doteq \dot{z}_L + \eta\dot{\varphi}_{x,L} - \xi\dot{\varphi}_{y,L}, \quad g = 1,\ldots,8. \tag{34}$$

According to (26), (27), the lateral velocities of the cell centres are

$$\dot{x}_{j,g} = \sum_l \sum_k -k\omega_l(\overline{x}_{j,g,l}^{(k)}\sin k\omega_l t + \overline{\overline{x}}_{j,g,l}^{(k)}\cos k\omega_l t), \tag{35}$$

$$\dot{y}_{j,g} = \sum_l \sum_k -k\omega_l(\overline{y}_{j,g,l}^{(k)}\sin k\omega_l t + \overline{\overline{y}}_{j,g,l}^{(k)}\cos k\omega_l t), \tag{36}$$

$j = 1,2,3$, $g = 1,\ldots,8$. The criterion of the FR cladding fretting wear can be expressed using the work of friction forces during the representative time interval $t \in \langle t_1, t_2\rangle$ calculated for the contact force $N_{j,g}(d_{j,r,g})$ and friction coefficient $f(c_{j,g})$. The slip velocities in particular contact points are

$$c_{j,g} = \sqrt{c_{j,t,g}^2 + c_{j,z,g}^2}, \quad j = 1,2,3, \quad g = 1,\ldots,8. \tag{37}$$

The *friction work* in contact points can be written as

$$W_{j,g} = \int_{t_1}^{t_2} f(c_{j,g})|N_{j,g}(d_{j,r,g})c_{j,g}|\,\mathrm{d}t, \quad j = 1,2,3, \quad g = 1,\ldots,8. \tag{38}$$

The *fretting wear* in grams of the FR cladding in particular contact points during the time interval $t \in \langle t_1, t_2\rangle$ can be expressed as

$$m_{j,g} = \mu W_{j,g}, \quad j = 1,2,3, \quad g = 1,\ldots,8, \tag{39}$$

where μ [g/J] is experimentally obtained fretting wear in grams (i.e. the loss of FR cladding mass in one contact surface generated by the friction work $W = 1$ [J] at the mean excitation frequency $\omega = \frac{1}{4}\sum_{l=1}^{4}\omega_l$ [12]). The small fluctuation of the angular velocity ω_l of particular main circulation pumps generates beating vibrations of the reactor component [18]. It is useful to choose the representative time interval for the calculation of the friction works as $t \in \langle t_0 - T/2, t_0 + T/2\rangle$, where t_0 is the time instant of the maximal beating vibration of the FA mounting plates and $T = 2\pi/\omega$. According to (38) and (39), the so called maximal periodic fretting wear is

$$m_{j,g}^{(T)} = \mu \int_{t_0-T/2}^{t_0+T/2} f(c_{j,g})|N_{j,g}(d_{j,r,g})c_{j,g}|\,\mathrm{d}t \quad j = 1,2,3, \quad g = 1,\ldots,8. \tag{40}$$

The hourly fretting wear in grams (the wear during one hour) can be approximately converted as

$$m_{j,g}^{(h)} = m_{j,g}^{(T)}\frac{3\,600}{T}. \tag{41}$$

6. Application

The presented method has been applied to the vibration analysis and fretting wear calculation of the FR in Russian FA (see Fig. 1). The FA mounting plates motion and displacements of

the spacer grid cell centres were precalculated using the global FA linearised model in the VVER 1000 type reactor for the excitation by pressure pulsations generated by main circulation pumps [20]. The basic mean excitation frequency corresponding to angular velocity of pumps is $\omega = 2\pi f$, $f = 16.6$ [Hz], the project values of cell stiffnesses are $k_r = 0.537 \cdot 10^6$ [N/m], $k_t = k_z = 10^6$ [N/m] and the static contact force representing the preloading between FR and particular spacer grid cells is assumed $N_0 = 10$ [N]. The friction-vibration characteristics of the contact forces between FR and spacer grid cells in the form (12) and (13) are approximated by the smooth functions (14) and (15) for the reference values of parameters $f_{st} = 0.2$, $f_d = 0.065$, $\varepsilon_f = 10^4$, $\varepsilon_k = 5\,000$ [s/m] and $d = 100$ [s/m]. For illustration, the sliding friction characteristics for different values of ε_f and d are displayed in Fig. 5.
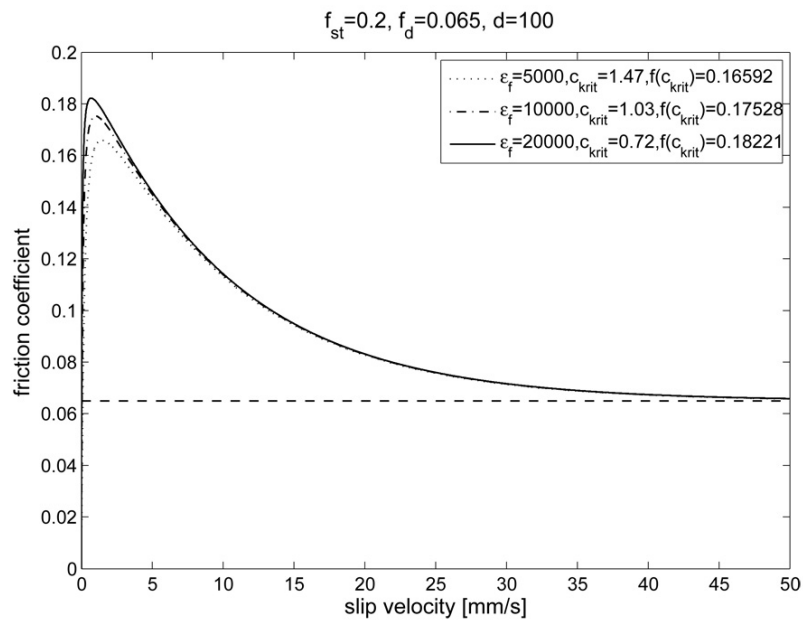
(a)
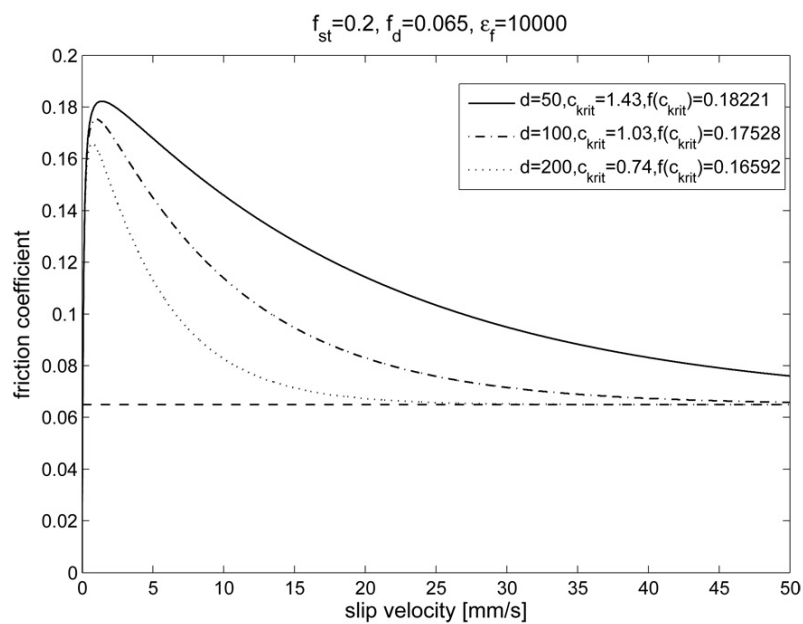
(b)

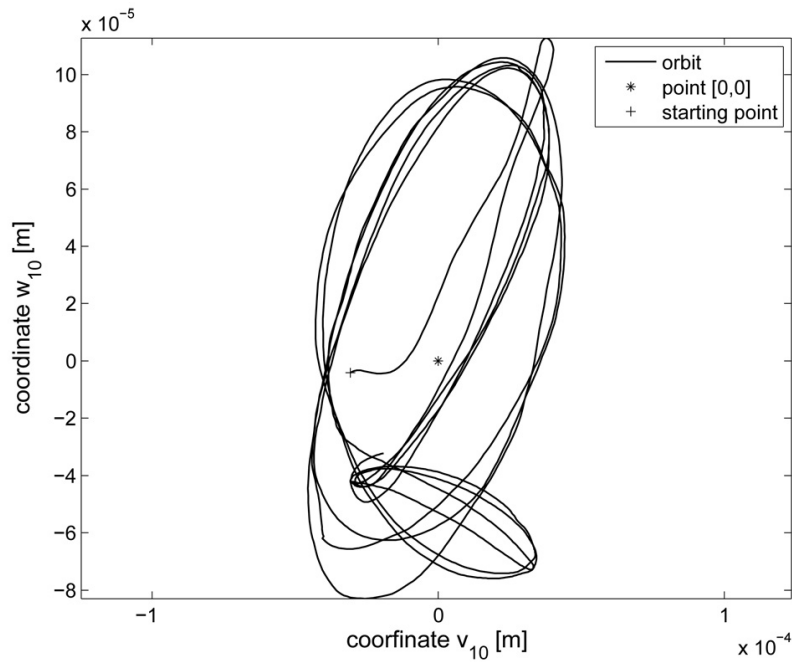Fig. 5. Friction characteristics for different ε_f (a) and d (b)

Fig. 6. Orbit of FR centre in nodal point $i = 10$

The *orbit of FR centre* in the nodal point $i = 10$ (located approximately in the FR middle) in the time interval $t \in \langle 19.9, 20.1 \rangle$ [s] at $t_0 = 20$ [s] of the maximal FA beating vibration is presented in Fig. 6. The three orbit loops correspond to three harmonic components ($k = 1, 2, 3$) of the coolant pressure pulsations considered in the kinematic excitation in (23).

For illustration, the time behaviour of the *slip velocities* $c_{1,g}$ in contact points of FR with the first cell at the level of spacer grids $g = 1, 4, 8$ is presented in Fig. 7. As evident, the maximal slip velocities increase with increasing distance of the spacer grid from the lower FA mounting plate. The well apparent stick states are repeated in contact points with the upper-most spacer
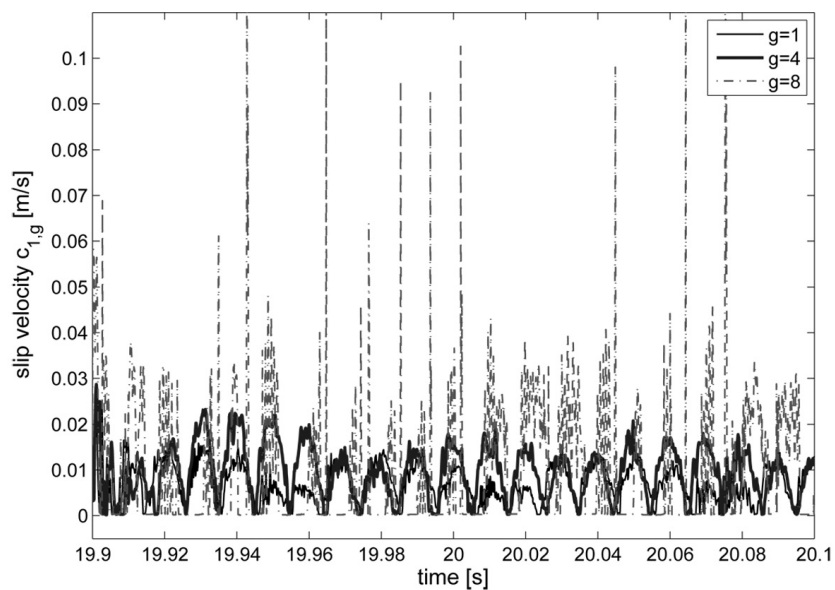

Fig. 7. Slip velocity $c_{1,g}$

grid $g = 8$. The time behaviour of the *normal contact force* $N_{1,g}$ at the same level of spacer grid is depicted in Fig. 8. The maximal normal contact forces are in contact points of FR with the lowest spacer grid cells (for $g = 1$). The *hourly fretting wear* of the FR cladding in all contact points with SG cells is shown in Fig. 9 for the face value $\mu = 10^{-9}$ [g/J] and the reference values of all parameters.
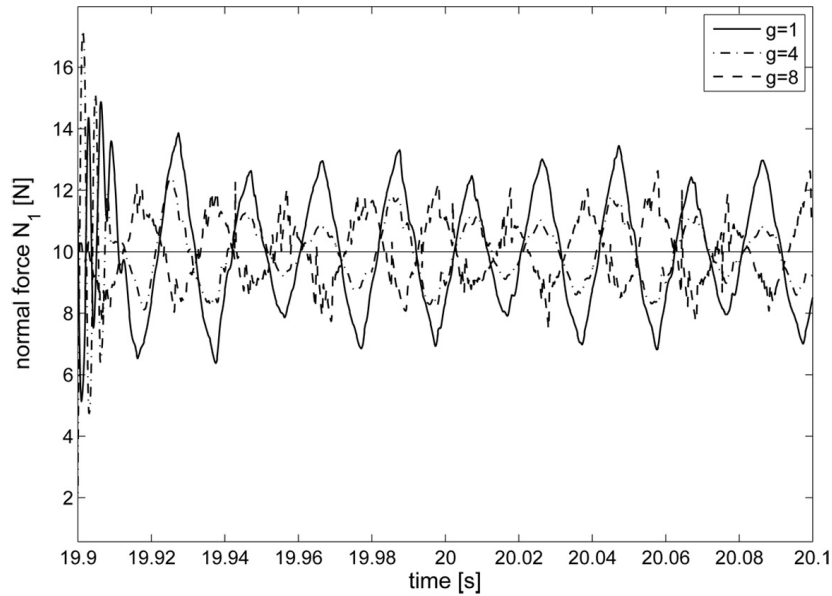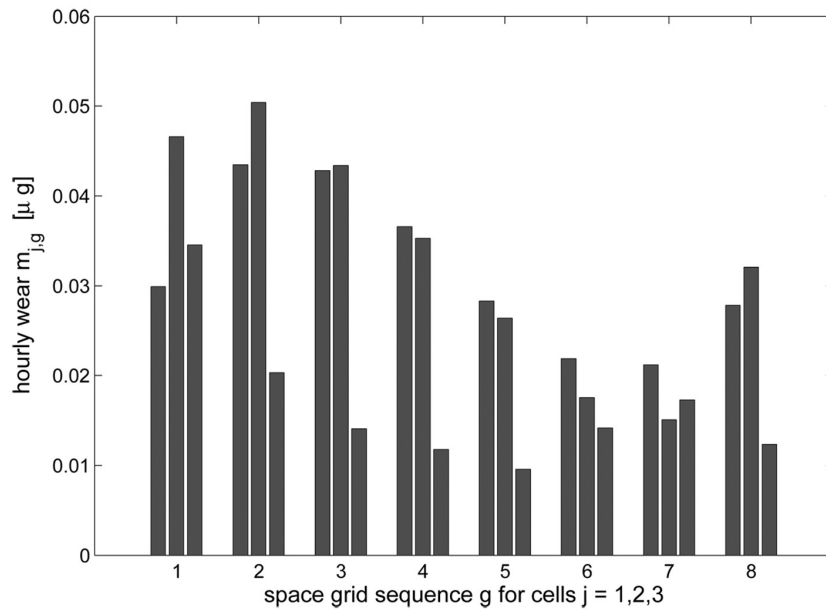

Fig. 8. Normal contact force $N_{1,g}$

Fig. 9. Hourly fretting wear

7. Conclusion

The main objective of this paper is to present a new basic method for the calculation of friction-vibration interactions of fuel rods in a nuclear fuel assembly. The method is based on mathematical modelling and computer simulation of nonlinear vibrations of fuel rods interacting

with spacer grid cells inside the fuel assembly skeleton. The contact forces include three possible states depending on deformations of cells and slip velocities. The developed software in Matlab code is designed in such a way that it enables the calculation of fuel rod deformations, slip velocities and friction works in all fuel rod contact points with spacer grid cells. The fuel rod and spacer grid vibrations are kinematically excited by the fuel assembly support plates motion caused by pressure pulsations generated by the main circulation pumps. The friction works can be used for the prediciton of fretting wear of the Zr fuel rod cladding. The presented method was applied for the case of fuel rods in the Russian TVSA-T fuel assembly in the VVER-1000 type reactor in the Czech nuclear power plant Temelín.

Acknowledgements

References

[1] Arkadov, G. V., Pavelko, V. I., Usanov, A. I., Vibro-acoustic diagnostics of VVER reactor, Energoatomizdat, Moscow, 2004. (in Russian)

[2] Blau, P. J., Friction science and technology: Form concepts to applications (second edition), CRC Press, Boca Raton, London, New York, 2009.

[3] Blau, P. J., A multistage wear model for grid-to-rod fretting of nuclear fuel rods, Wear 313 (1–2) (2014) 89–96.

[4] Hlaváč, Z., Zeman, V., Vibration of nuclear fuel assemblies: Modelling, methods, applications, LAP Lambert Academic Publishing, Saarbrücken, 2013.

[5] Kim, H. K., Lee, Y. H., Lee, K. H., On the geometry of the fuel rod supports concerning a fretting wear failure, Nuclear Engineering and Design 238 (12) (2008) 3 321–3 330.

[6] Kim, K. T., A study on the grid-to-rod fretting wear-induced fuel failure observed in the 16×16KOFA fuel, Nuclear Engineering and Design 240 (4) (2010) 756–762.

[7] Kim, K. T., The effect of fuel rod supporting conditions on fuel rod vibration characteristics and grid-to-rod fretting wear, Nuclear Engineering and Design 240 (6) (2010) 1 386–1 391.

[8] Lee, Y. H., Kim, H. K., Effect of spring shapes on the variation of loading conditions and the wear behaviour of the nuclear fuel rod during fretting wear tests, Wear 263 (16) (2007) 451–457.

[9] Lee, Y. H., Kim, H. K., Fretting wear behaviour of a nuclear fuel rod under a simulated primary coolant condition, Wear 301 (1–2) (2013) 569–574.

[10] Lu, R., Karoutas, Z., Sham, T. L., CASL virtual reactor predictive simulation: Grid-to-rod fretting wear, The Journal of The Minerals, Metals & Materials Society 63 (8) (2011) 53–58.

[11] Pečínka, L., Stulík, P., The experimental verification of the reactor WWER 1000/320 dynamic response caused by pressure pulsations generated by main circulation pumps, Proceedings of the Colloquium Dynamic of Machines 2008, Institut of Thermomechanics AS CR, 2008, pp. 87–94.

[12] Pečínka, L., Svoboda, J., Zeman, V., Fretting wear of the Zr-fuel rod cladding, Proceedings of the 22nd International Conference of Nuclear Engineering ICONE22, ASME, 2014, pp. V001T03A027.

[13] Rubiolo, P. R., Probabilistic prediction of fretting wear damage of nuclear fuel rods, Nuclear Engineering and Design 236 (14–16) (2006) 1 628–1 640.

[14] Sextre, W., Dynamic contact problems with frictions: Models, methods, experiments and applications, Springer, Berlin, Heidelberg, 2007.

[15] Voldřich, J., Modelling of the three-dimensional friction contact of vibrating elastic bodies with rough surfaces, Applied and Computational Mechanics 3 (1) (2009) 241–252.

[16] Yan, J., Yuan, K., Tatli, E., Karoutas, Z., A new method to predict Grid-To-Rod Fretting in a PWR fuel assembly inlet region, Nuclear Engineering and Design 241 (8) (2011) 2 974–2 982.

[17] Zeman, V., Hlaváč, Z., Modelling of WWER 1000 type reactor vibration by means of decomposition method, Book of Extended Abstracts – Engineering Mechanics 2006, Institut of Theoretical and Applied Mechanics AS CR, Prague, 2006, pp. 444–445.

[18] Zeman, V., Hlaváč, Z., Dynamic response of VVER 1000 type reactor excited by pressure pulsations, Engineering Mechanics 15 (6) (2008) 435–446.

[19] Zeman, V., Hlaváč, Z., Vibration of the package of rods linked by spacer grids, Proceedings of the 10th International Conference on Vibration Problems (Vibration Problems ICOVP 2011), Springer, 2011, pp. 227–233.

[20] Zeman, V., Hlaváč, Z., Dynamic response of nuclear fuel assembly excited by pressure pulsation, Applied and Computational Mechanics 6 (2) (2012) 219–230.

[21] Zeman, V., Hlaváč, Z., Prediction of the nuclear fuel rod abrasion, Applied and Computational Mechanics 7 (2) (2013) 235–250.

[22] Zeman, V., Dyk, Š., Hlaváč, Z., Mathematical modelling of nonlinear vibration and fretting wear of the nuclear fuel rods, Archive of Applied Mechanics 86 (4) (2016) 657–668.